

Information theory and robotics meet to study predator-prey interactions

Cite as: Chaos **27**, 073111 (2017); <https://doi.org/10.1063/1.4990051>

Submitted: 04 April 2017 . Accepted: 12 June 2017 . Published Online: 18 July 2017

 Daniele Neri, Tommaso Ruberto, Gabrielle Cord-Cruz, and  Maurizio Porfiri

COLLECTIONS

 This paper was selected as Featured



View Online



Export Citation



CrossMark

ARTICLES YOU MAY BE INTERESTED IN

[Detecting switching leadership in collective motion](#)

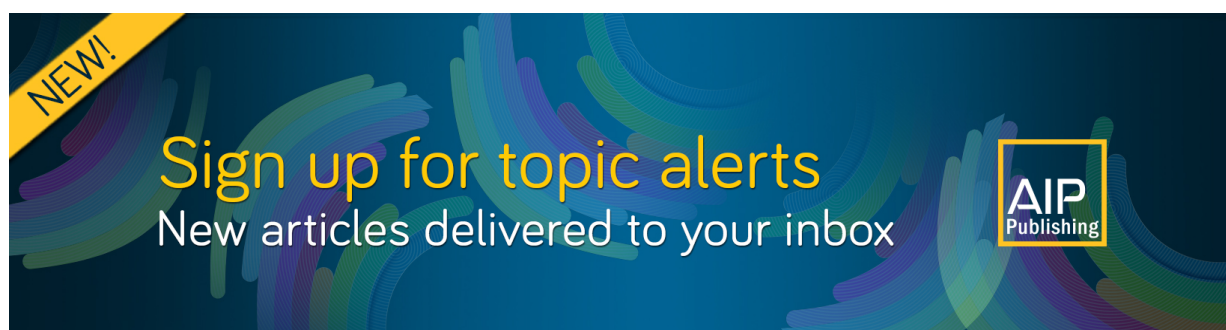
Chaos: An Interdisciplinary Journal of Nonlinear Science **29**, 011102 (2019); <https://doi.org/10.1063/1.5079869>

[Detecting causality in policy diffusion processes](#)

Chaos: An Interdisciplinary Journal of Nonlinear Science **26**, 083113 (2016); <https://doi.org/10.1063/1.4961067>

[Modeling back-relaxation in ionic polymer metal composites: The role of steric effects and composite layers](#)

Journal of Applied Physics **123**, 014901 (2018); <https://doi.org/10.1063/1.5004573>



Information theory and robotics meet to study predator-prey interactions

Daniele Neri,^{a)} Tommaso Ruberto,^{a)} Gabrielle Cord-Cruz, and Maurizio Porfiri^{b)}

Department of Mechanical and Aerospace Engineering, New York University, Tandon School of Engineering, 6 MetroTech Center, Brooklyn, New York 11201, USA

(Received 4 April 2017; accepted 12 June 2017; published online 18 July 2017)

Transfer entropy holds promise to advance our understanding of animal behavior, by affording the identification of causal relationships that underlie animal interactions. A critical step toward the reliable implementation of this powerful information-theoretic concept entails the design of experiments in which causal relationships could be systematically controlled. Here, we put forward a robotics-based experimental approach to test the validity of transfer entropy in the study of predator-prey interactions. We investigate the behavioral response of zebrafish to a fear-evoking robotic stimulus, designed after the morpho-physiology of the red tiger oscar and actuated along preprogrammed trajectories. From the time series of the positions of the zebrafish and the robotic stimulus, we demonstrate that transfer entropy correctly identifies the influence of the stimulus on the focal subject. Building on this evidence, we apply transfer entropy to study the interactions between zebrafish and a live red tiger oscar. The analysis of transfer entropy reveals a change in the direction of the information flow, suggesting a mutual influence between the predator and the prey, where the predator adapts its strategy as a function of the movement of the prey, which, in turn, adjusts its escape as a function of the predator motion. Through the integration of information theory and robotics, this study posits a new approach to study predator-prey interactions in freshwater fish. *Published by AIP Publishing.* [<http://dx.doi.org/10.1063/1.4990051>]

Identifying causal relationships in coupled dynamical systems from their time series is a ubiquitous problem in science and engineering. Through the information-theoretic concept of transfer entropy, researchers have recently unraveled functional connectivity patterns in the brain, identified climate networks all around the globe, and explained the process of policy making in the United States of America. Whether transfer entropy could bestow similar advancements in the field of animal behavior is yet to be fully verified. This study puts forward a new robotics-based approach to control information flow in predator-prey interactions and test the validity of transfer entropy to identify causal influences. We demonstrate the possibility of identifying the influence of a preprogrammed robotic predator on the behavior of a zebrafish from their movements. When the robotic predator is replaced with a live predator, we show that a one-directional information flow is abolished. The visual interaction between the live predator and the focal subject causes a positive feedback loop, where the predator is vigilant of the behavior of its potential prey, which, in turn, displays an avoidance response. This interdisciplinary study constitutes a first, necessary step toward the systematic application of transfer entropy to answer open questions in animal behavior, such as the process of information spreading in social groups during predator attacks.

I. INTRODUCTION

Information is a very useful commodity for animals, which is why they dedicate time and energy in obtaining it throughout their life.¹ Through their senses and perception, animals can access and process information about their surroundings.^{1–3} This form of adaptive behavior⁴ plays a crucial role in finding optimal survival strategies,⁵ such as finding a mating site, identifying a foraging site, and recognizing a predatory threat.⁶ The precise and objective quantification of the information that is used by animals to make decisions is important to explain causal relationships at the basis of animal behavior. For example, when a social group is attacked by a predator, critical information is likely to be transmitted nonverbally from the predator to some of the prey, which will then spread the information throughout the group to trigger their escape; at the same time, information will be transmitted from the prey to the predator, which will adjust its strategy as a function of the group dynamics.⁶

Apprehending this complex information flow across physical and temporal scales is an open challenge, which has attracted the interest of biologists, physicists, and engineers in the last two decades.^{7–11} The field of information theory¹² offers a potent framework to investigate information flow in the animal world, enabling the inference of causal relationships from time-series of individual and collective behavior. While the origins of this field are rooted in communication theory, due to the seminal work of Shannon,¹³ information theory has fostered major breakthroughs in statistical mechanics, probability theory, and algorithm complexity, to name just a few technical domains.¹² Only recently, the animal behavior community has looked at information theory

^{a)}D. Neri and T. Ruberto contributed equally to this work.

^{b)}Author to whom correspondence should be addressed: mporfiri@nyu.edu.
Tel.: +1-646-997-3681. Fax: +1-646-997-3532.

for supporting research in psychopharmacology,¹⁴ ecology,¹ vocal communication,¹⁵ and evolution.¹⁶

Among the vast array of mathematical tools that information theory puts forward to study information flow in dynamical systems,¹⁷ transfer entropy has emerged as a promising method for unraveling causal relationships from raw data, without the need for a background model and allowing for the occurrence of nonlinear interactions.¹⁸ This method has been successfully applied in neuroscience,^{19,20} climate networks,^{21,22} global networks of financial companies,²³ physiology,²⁴ and policy diffusion.^{25,26} Transfer entropy allows researchers to identify causal relationships between two coupled dynamical systems by measuring the reduction in the level of uncertainty—entropy—in predicting the state of a system given the knowledge of the past of the other system.²⁷ In the context of animal behavior, we could say, that a stimulus causes a certain response of the animal, if the uncertainty in predicting the future response in the animal from its past is reduced when considering the stimulus.

For example, in the analysis on pairs of bats from flying swarms by Orange and Abaid,²⁸ transfer entropy, measured in terms of the inverse radius of curvature derived from the subjects' trajectory, was used to explain positional preference of leaders in a group. Experimental results presented therein suggested that a higher amount of information is transferred from the foremost located individual to the subject in the rear, supporting the hypothesis that leading individuals should be located ahead of the rest of the group, toward the group direction. In the study of interactions between a predator and a prey fish by Hu *et al.*,²⁹ transfer entropy is instead scored in terms of the position of the subjects. Experimental findings presented therein indicate that a net flow of information is elicited from the predator to the prey, thereby suggesting a higher apprehension of the prey regarding the predator's movement.

While transfer entropy holds promise to advance our understanding of animal behavior in response to external stimuli, as demonstrated through computer simulations,^{30,31} the experimental reliability of causal relationships inferred through transfer entropy remains elusive. Given a set of experimental data, results could vary according to several parameters, such as the choice of the variable to score transfer entropy on (for example the inverse of the radius of curvature in Ref. 28 and the position in Ref. 29), the number of bins used to discretize the selected variable for the estimation of the probability density functions (along with the binning method itself), the frame rate of the data acquisition, and the duration of the experimental observations.^{17,18,32} Therefore, it is necessary to establish experimental approaches to validate the use of this theoretical-construct, prior to testing scientific hypotheses on unknown biological dependencies. Here, we propose a robotics-based experimental paradigm to systematically control for the direction of information flow, thereby offering reliable data on which we could test the validity of transfer entropy in the study of predator-prey interactions.

Robotics is rising as a popular and effective method to engineer artificial stimuli in animal behavior.^{33–38} Robotics allows for generating customizable, controllable, and repeatable stimuli in laboratory environments, which can be used

to evoke a wide array of emotional responses in experimental subjects. In the experiments presented here, we used a 3D-printed replica of a red tiger oscar fish (*Astronotus ocellatus*) as a visual stimulus to study the antipredatory response in zebrafish (*Danio rerio*). Different from previous work on the use of fear-evoking robots,^{39,40} where the replicas were anchored at a fixed location of the tank while only beating their tail, our novel platform is able to maneuver the 3D-printed replica along predetermined and customizable trajectories. Zebrafish was selected for the experiment based on its translational value in medicine,^{41–45} which has favored the development of several robotics-based experimental paradigms to study its behavior.³⁵ The antipredatory response in zebrafish shares analogies with anxiety- and fear-related responses in humans.^{46–48} The presentation of predatory stimuli, either sympatric or allopatric,⁴⁹ has been shown to a valid stimulus to evoke fear response in zebrafish, enhancing associated neuroendocrinal pathways, such as cortisol expression.⁵⁰

By decoupling the trajectory of the predatory stimulus from the response of the zebrafish through our robotics-based platform, we aimed at establishing a unidirectional flow of information for probing the information-theoretic construct of transfer entropy. Similar to the work of Hu *et al.*,²⁹ we studied information flow in terms of the position of the stimulus and the zebrafish in a circular arena, where the robotic stimulus was preprogrammed to maneuver along circular trajectories using a robotic arm in the central portion of the arena. A cam system was utilized to induce oscillatory movements, reminiscent of predator swimming. The live fish was free to swim in the outer annular region of the arena, and a transparent panel was used to physically separate the stimulus from the focal subject. To control for the visual stimulus presented to the focal subject, we performed two experimental conditions in which: (i) the 3D-printed replica was not present, such that the live subject might only perceive the presence of the robotic arm, and (ii) the entire robotic platform was removed, such that the central region of the arena was empty. To demonstrate the use of transfer entropy in supporting scientific research, we also studied the response of zebrafish to a live predator, swimming in the central portion of the arena. The two-dimensional positions of the stimuli and focal subjects were acquired for every trial using our tracking software,³⁹ which allows for refined resolution of movements.

If transfer entropy were a valid tool for identifying causal relationships, then we should find a one-directional information flow from the robotic predator to the live zebrafish, such that the behavior of zebrafish will be caused by the robotic stimulus and not vice-versa. Upon validating transfer entropy in this context, we expected to shed light on the interaction between the live predator and zebrafish. While it is reasonable to anticipate that the live predator will adjust its behavior as a function of zebrafish, and zebrafish will, in turn, change its behavior as a function of the predator, it is difficult to predict the strength of each of these relationships.^{51,52} Once validated on the robotics-based platform, we expected to answer this question. To place the answer to this question in a meaningful biological context, we integrated the information-theoretic analysis with a refined analysis of

the positional preference and activity of the stimulus and the zebrafish. Finally, we assessed the consistency of the responses evoked by the robotic and live stimuli over time.

II. MATERIALS AND METHODS

A. Ethics statements

Experiments were performed in accordance with relevant guidelines and regulations, and were approved by the University Animal Welfare Committee (UAWC) of New York University under protocol number 13-1424 (Robotics based experimental paradigms to study social behavior, reward pathways, and their development adjustments in fish).

B. Animals

In this study, we utilized 40 adult wild-type zebrafish (*Danio rerio*) as focal subjects, each with an approximate body length of 3 cm. Fish were purchased from an online vendor (LiveAquaria.com, Rhinelander, WI, USA) in June 2016 and were housed in four 10 gallons (37.8 l) tanks of a vivarium (Pentair Aquatic Eco-Systems Locations, Cary, NC, USA), each containing up to 10 fish. Water temperature was kept at $25 \pm 1^\circ\text{C}$ and water pH at 7.2. Fish were exposed to a 12-h light and 12-h dark period.⁵³ The zebrafish were fed with flake food (Hagen Corp. Nutrafin max, Mansfield, MA, USA) from 6:00 to 7:00 pm every day.

Two red tiger oscar fish (*Astronotus ocellatus*), approximately 7.5 cm in body length, were used as predatory stimuli. Red tiger oscar fish were purchased from the same online vendor used for the zebrafish. They were housed in 31 gallons (115 l) tanks and kept at the same light period and water parameters as the zebrafish. Red tiger oscar fish were fed with floating pellet food (Kyorin Co., Hikari Cichlid Cichlid Gold) twice a day, from 1:00 to 2:00 pm, and from 6:00 to 7:00 pm every day. All of the fish were given a period of 12–15 days of habituation before experiments.

C. Apparatus

The experimental apparatus consisted of a circular arena (45 cm radius), delimited by an aluminum ring covered with white contact paper that was placed in the center of a rectangular tank of dimensions $120 \times 120 \times 20$ cm (length, width, and depth). The water depth was maintained at 12 cm. A cylindrical Plexiglas stimulus tank with radius 12.7 cm and height 50 cm was used to physically separate the stimulus from the focal subjects during the experiments (Fig. 1). Holes were drilled in the bottom part of the stimulus tank to ensure the same water properties for the live stimuli and the focal subjects.

A high-resolution Flea3 USB camera (Point Grey Research Inc., Richmond, British Columbia, Canada) was mounted above the experimental setup at 100 cm from the water surface. Two Logitech web cameras (Logitech, Newark, CA, USA) were mounted laterally to the Flea3 camera to record the trials from a different perspective. The webcams were triggered simultaneously through a Linux shell script to record near-synchronous videos. For the condition

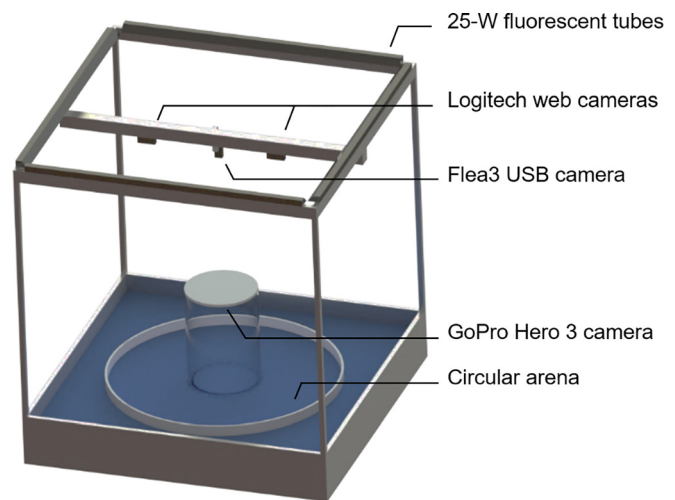


FIG. 1. Sketch of the experimental apparatus. Black curtains are not shown. The GoPro used for the scoring the behavior of the live predator condition was placed under the lid covering the stimulus tank.

with the live red tiger oscar, a GoPro Hero 3 camera (GoPro Inc., San Mateo, CA, USA) was mounted on an acrylic disk placed over the stimulus tank as a lid, facing the inside. The GoPro camera was used to record the position of the live stimulus. All the cameras were set at an acquisition frequency of 30 frames per second (fps).

Four 25-W fluorescent tubes (All-Glass Aquarium, Franklin, WI, USA) were placed 100 cm above the rectangular tank to illuminate the experimental apparatus. The experimental apparatus was surrounded by black curtains to reduce any possible disturbance from the surrounding environment.

B. Replica and robotic platform

The biologically inspired replica of the red tiger oscar [Fig. 2(a)] was based on the replica proposed by Ladu *et al.*³⁹ The design of the replica was scaled in SolidWorks (Dassault Systèmes SolidWorks Corp., Waltham, MA, USA) to match the live oscar fish proportions [Fig. 2(b)]. Differently from Ladu *et al.*,³⁹ the replica was composed of a single rigid body and was fabricated using a Dimension Elite 3D printer (Stratasys Ltd., Eden Prairie, MN, USA) with acrylonitrile butadiene styrene (ABS) thermoplastic. The replica was painted with non-toxic paint (Krylon, Krylon Products Group, Cleveland, OH, USA) to mimic the appearance and color pattern of the live red tiger oscar. Then, the 3D printed replica was attached to an acrylic transparent rod and connected to the robotic platform.

The robotic platform was conceived to afford the motion of the replica in the stimulus tank. The platform was also designed in SolidWorks, and it was fabricated using acrylic elements and 3D-printed parts [Fig. 3(a)]. It consisted of a two-piece master frame, an Arduino Uno microcontroller (Arduino Uno, Arduino, Italy), a support case for the Arduino Uno microcontroller, a stepper motor (Adafruit, New York City, NY, USA), a cam system, and a rotating acrylic disk, which was covered with white contact paper. The master frame, cam system, and support case for the Arduino Uno microcontroller were fabricated using a Dimension Elite 3D

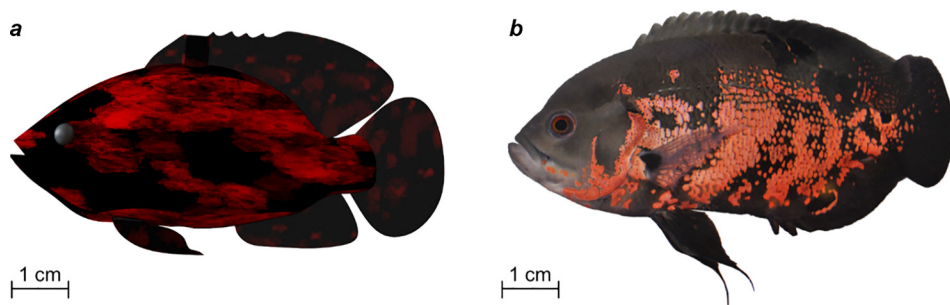


FIG. 2. Biologically inspired replica of a red tiger oscar (a) and its live counterpart (b).

printer with ABS thermoplastic. The master frame was fixed to an acrylic ring placed on top of the stimulus tank.

The cam system [Fig. 3(b)] consisted of an elliptical cam follower and a cam frame, which was fixed to the master frame using nuts and bolts. The cam follower measured 3.9 cm and 1 cm along the major and minor axes, respectively. The cam frame had an overall diameter of 16.5 cm and was designed to display a sinusoidal pattern with 12 peaks (peak-to-peak distance of 4.3 cm), each with an amplitude of 0.5 cm. A hole was drilled through the rotating acrylic disk, such that the acrylic rod could pass through it and rotate together with it. The bottom of the rod was connected to the replica, while the top was attached to the elliptical cam follower. An elastic rubber band was used to ensure form-fitting contact between the cam frame and cam follower. A stepper motor, connected to the acrylic disk via a screw and coupler, was used to actuate the rotating disk. The rotation of the disk, in turn, produced the circular trajectory of the rod along with brief sinusoidal oscillations about its axis, which were intended to mimic the oscillatory movement of a real predator.

An Adafruit (Arduino, Italy) motor shield was mounted onto the Arduino Uno microcontroller, which was used to drive the stepper motor. The Arduino Uno microcontroller was connected to a computer using a USB cable and was used to operate the robotic platform through a script coded in MATLAB (MathWorks, Natick, MA, USA).

To reproduce the movement of a live predator, we performed pilot trials on the two red tiger oscar. Each of the oscar fish was individually placed inside the cylindrical tank filled with 12 cm of water. No zebrafish were involved in the two pilot experiments. A lid was placed on top of the cylindrical tank with the GoPro Hero 3 camera mounted on the part of the lid facing the tank to capture videos of the oscar fish. Twenty minutes of footage were recorded for each trial, with the first 10 min considered as habituation. The data from the latter 10 min of the videos were analyzed to measure the behavior of oscar fish. Based on these observations, we found that the predators performed very small movements in the stimulus tank at high variable speed, with an average distance covered of approximately 124.6 cm over 10 min. These data were inputted in the MATLAB code to standardize the presentation of the robotic stimulus.

The robotic platform was programmed to execute a start-and-stop motion along a predetermined trajectory. To mimic the variations in the speed of the live predator, the platform was programmed to piece-wise change the motor speed in the trial. Specifically, in each trial, the trajectory consisted of a sequence of movements at a constant angular speed of different durations, separated by short pauses. Using the MATLAB-Arduino package, a matrix was created, where each column specified a different parameter of the movement: angular speed, angular distance to cover, and pause time. Each of the rows corresponded to a different combination of these three parameters, and the total number

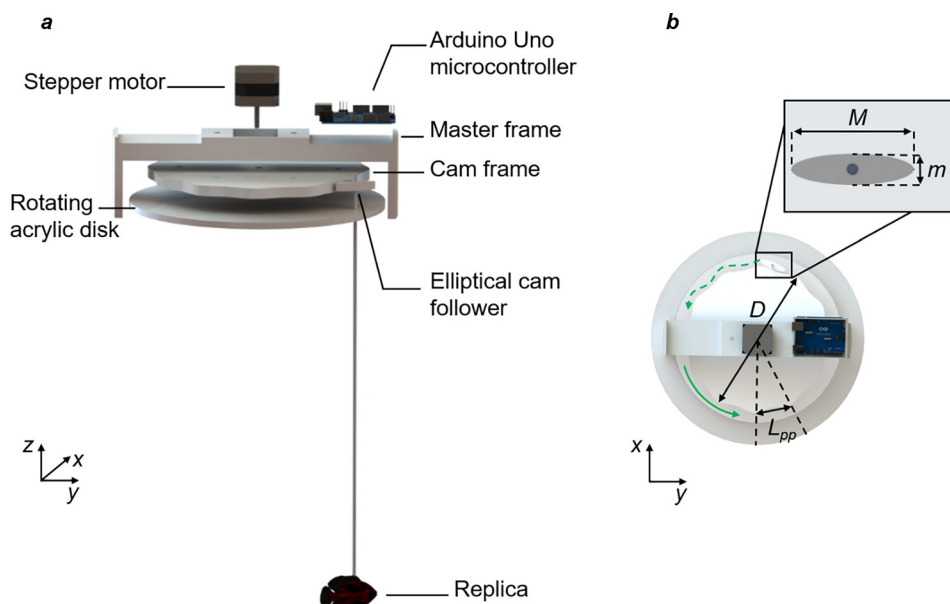


FIG. 3. Exploded schematics (a) and illustration of the working principle of the robotic platform from a top view (b), depicting the cam frame diameter (D), peak-to-peak distance (L_{pp}), and a close-up of the elliptical cam follower. In the close-up, M and m are the major and the minor axes, respectively. The trajectory of the replica is illustrated as a dashed green line, while the motion of the rotating acrylic disk is illustrated as a solid green line.

of rows was chosen as 200 to cover the entirety of each trial. The angular speed was randomized between 0 and 50 rotations per minute (rpm) and the angular distance was randomized between 0 and 50 steps, where one step was equivalent to 1.8° . The pause time was also randomized in a range between 0 and 100 s. Finally, the stepper motor was programmed to implement the start-and-stop motion for the entire duration of the trial by randomly selecting a new row of the matrix after the conclusion of the previous command.

E. Procedure

All experiments were conducted in July 2016. Each zebrafish was tested once, while each of the red oscar tiger fish was utilized for five trials. Fish were handled with different hand nets, one for zebrafish and one for oscar fish. Four experimental conditions were considered in this study. Specifically, we performed a condition using a live predator (“Live” condition) as the stimulus; a condition in which the live predator was replaced by the robotic replica (“Replica” condition); a condition with no replica attached to the robotic platform (“CTRL Replica” condition); and, finally, a condition in which no stimulus was presented to the fish, leaving the stimulus tank empty (“CTRL Live” condition). For each condition, we performed 10 trials and each trial consisted of 21 min, comprising 10 min of habituation and 10 min of experimental observation, with 1 min in between of them.

Before starting each trial, a black tarp was placed around the stimulus tank to hide the stimulus from the zebrafish and, for Live condition, also hide the zebrafish from the predator. The tarp was removed at the end of the habituation time. Since the removal of the black tarp caused ripples on the surface of the water, which challenged the tracking software, we decided to interpose one minute between the habituation and the experimental observation. For each trial, all the 21 min were video recorded, and only the last 10 min—experimental observation—were analyzed.

In condition Live, one red oscar tiger fish was released in the stimulus tank. The black tarp was placed around the stimulus tank, the GoPro camera was started manually, and the acrylic disk with the camera attached to it was placed on top of the stimulus tank. Then, one focal fish was picked randomly and released in the circular arena. All the other cameras started recording right after the release of the focal subject. After the trial, both the focal subject and red tiger oscar fish were located in separate holding tanks (see [supplementary material](#) videos 1 and 2). The two red tiger oscar fish were alternated between trials, such that each was used in five trials. In condition CTRL Live, the same procedure was used but no oscar tiger was placed in the stimulus tank (see [supplementary material](#) video 3).

In condition Replica, the robotic platform with the predator replica attached to the acrylic rod replaced the red oscar tiger fish as the predatory stimulus in the stimulus tank. Similar to the previous conditions, a focal subject was picked randomly and released in the circular arena. The cameras started recording within a second after the focal subject release, and then, the robotic platform was started in MATLAB. At the end of the trial, the robotic platform was

stopped, and the focal subject was removed from the experimental setup and placed in a separate holding tank of the vivarium (see [supplementary material](#) video 4). In condition CTRL Replica, no replica was attached to the rod actuated by the robotic platform. The same procedure used in condition Replica was followed for this experimental condition (see [supplementary material](#) video 5).

Two sessions of trials were performed during one experimental day, with five trials in the morning from 9:00 am to 1:00 pm, and five in the afternoon from 2:00 to 6:00 pm, for a total of 10 trials per day. The order of the experimental conditions was randomized and balanced throughout each experimental day.

F. Data analysis

All the recorded videos were first converted into image frames prior to the analysis. The videos of the live predator were individually rotated and synchronized to match the videos of the zebrafish from the respective trials. Specifically, videos were edited with the freeware VLC media player (VideoLan, Paris, France), using points of the experimental tank visible from both the GoPro and the Flea3 cameras as a reference for the rotation, while synchronization was achieved by matching the image frames of the removal of the black tarp from the stimulus tank.

Finally, the image frames were post-processed through automated custom-made tracking software that identified the zebrafish position. Specifics of the tracking software can be found in previous works from our group.⁵⁴ The trajectories of the stimuli in the Replica and CTRL Replica conditions were estimated by tracking the position of the elliptical cam frame (Fig. 4). The distance covered by the robotic stimuli during the twenty trials was 121.7 ± 73.6 cm (mean \pm standard deviation), which was highly comparable with the distance covered by the red tiger oscars in the two pilot experiments (124.6 cm).

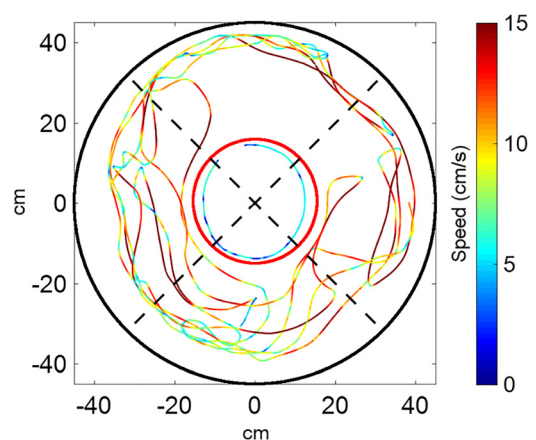


FIG. 4. Illustration of the binning used to compute transfer entropy superimposed to the trajectories of zebrafish and the robotic replica extracted from a portion of a trial from the Replica condition. The red circle represents the stimulus tank; the black circle identifies the experimental arena; dashed black lines are the virtual subdivision of the circular arena into four equal 90° slices. Trajectories are colored to illustrate fish and replica instantaneous speed, with reference to the color bar on the right.

The information-theoretic construct of transfer entropy²⁷ was used to measure the flow of information between zebrafish and stimulus. Briefly, given two stationary stochastic processes X and Y (that is, positional data of zebrafish and stimulus in our study) transfer entropy²⁷ from Y to X is defined as

$$T_{Y \rightarrow X} = \sum_{x_{t+1}, x_t, y_t} p(x_{t+1}, x_t, y_t) \log_2 \frac{p(x_{t+1}|x_t, y_t)}{p(x_{t+1}|x_t)}, \quad (1)$$

where x_t and x_{t+1} are the realization of X at time step t (present) and $t+1$ (future), respectively; y_t is the realization of Y at time step t ; $p(x_{t+1}, x_t, y_t)$ is the joint probability distribution of X at the future time step, X at the present time step, and Y at the present time step; $p(x_{t+1}|x_t, y_t)$ indicates the conditional probability of X at the next time step given the present values of X and Y ; $p(x_{t+1}|x_t)$ indicates the conditional probability of X at the future time step given only the present value of X ; and, finally, Σ identifies summation over all the possible realizations of X at the future time step, X at the current time step, and Y at the current time step. The summation could be replaced with an integral for stochastic processes taking continuous values; in our case, we binned position data in a finite number of classes such that the summation is always taken over the same sets.

Transfer entropy measures the reduction in the uncertainty of the prediction of the future of X from its present, due to the additional knowledge of the present of Y . In terms of conditional entropy, we may write $T_{Y \rightarrow X} = H(x_{t+1}|x_t) - H(x_{t+1}|x_t, y)$ where H indicates entropy, which clarifies the connection between transfer entropy and reduction in uncertainty, measured through Shannon's entropy. If Y does not influence X , then $p(x_{t+1}|x_t, y_t) = p(x_{t+1}|x_t)$ and transfer entropy is equal to zero. On the other hand, if Y influences X , the transfer entropy is positive, such that Y possesses some useful information about the future of X . By construction, transfer entropy is not symmetric,¹⁸ such that $T_{Y \rightarrow X}$ and $T_{X \rightarrow Y}$ could be compared to identify the dominant direction of information flow and unravel a causal relationship between the two processes. This step was specifically undertaken by computing the net transfer entropy for each condition, as the difference between the transfer entropy values from the fish to the stimulus and those in the opposite direction. Net transfer entropy was used as an indicator of causality, whereby nonzero net transfer entropy would imply causality.

Transfer entropy was computed from the angular coordinates θ_z and θ_s of the zebrafish and the stimulus, respectively, using Process_Network_v.1.4 software.⁵⁵ Transfer entropy computations were carried out using four equal bins of 90° (Fig. 4) and a time step equal to the acquisition period. The consistency of the identified causality was confirmed by systematically varying the bin size and the sampling frequency with respect to the reference values of four and 30 fps, respectively. Specifically, we computed net transfer entropy by varying the number of bins from 3 to 10, while holding the time step to the acquisition time, and by down-sampling the data until 1 fps.

For each condition, zebrafish activity was studied in terms of the distance travelled and average absolute turn rate. Spatial preference was scored in terms of the cumulative

distributions of the distance of the zebrafish from the center of the tank. For the three conditions where a stimulus was present (CTRL Replica, Live, and Replica conditions, respectively), we computed the distance travelled by the stimulus, the avoidance of the stimulus, and the number of crossings.

The distance travelled by the zebrafish and the stimulus was evaluated from the positions acquired by the software. The average absolute turn rate of zebrafish was evaluated from a central difference approximation of the turning angle based on the fish position.⁵⁶

The cumulative distribution of the distance of zebrafish from the center was studied by discretizing the difference between the radius of the circular arena and the radius of the stimulus tank (45 cm–12.7 cm = 32.3 cm) into 32 concentric rings of approximately 1 cm in width. Zebrafish radial coordinate with respect to the center of the tank was used for binning, resulting in one integer number between 1 to 32 for every frame, with 1 indicating the innermost and 32 the outermost ring. Bin frequencies were computed by dividing the number of frames scored in the ring by the total number of frames. Finally, we estimated the cumulative distributions of each condition from ring 1 to ring 32.

The avoidance of the stimulus and the number of crossings were calculated using a distance of three body lengths⁵⁷ from the stimulus (7.5 cm \times 3 = 22.5 cm). For each frame, a circle of radius 22.5 cm was centered at the location of the stimulus, defining a so-called “predator area.” Avoidance was computed as the percentage of time spent by zebrafish outside of the predator area in each trial. The number of crossings was computed as the number of times that the zebrafish traversed the predator area in each trial.

We also evaluated time effects in the distance travelled and average absolute turn rate of zebrafish. We scored each activity index for each minute of every trial and averaged the first three minutes (“first segment”) and the last three minutes (“last segment”). This procedure was chosen to analyze the behavior and activity of the focal subjects during the first third and last third of the trial.

Outliers were identified using interquartile range (IQR) \times 1.5 rule⁵⁸ applied to the distance traveled by the focal subjects. Two fish from the Replica condition were discarded from the analyses accordingly.

Distance travelled by zebrafish and average absolute turn rate of zebrafish were individually analyzed using a one-way analysis of variance (ANOVA) with the four conditions as the independent variable. One-way ANOVA was also used to compare avoidance of the stimulus, number of crossings, transfer entropy from fish to stimulus, and transfer entropy from stimulus to fish in the conditions involving a stimulus (CTRL Replica, Live, and Replica), with the three conditions as the independent variables. In order to analyze the avoidance of the stimulus with one-way ANOVA, we transformed the data using the *logit* function ($\log \frac{x}{1-x}$). The number of crossings was analyzed using a generalized linear model with negative binomial family distribution to ensure the best fit for a dataset composed of positive integer numbers. The model was tested using a likelihood ratio test by comparing it with a null model that does not contain the group factor. To assess the validity of our tests, every residual quantile-quantile plot was visually

inspected to ensure the normal distribution of the residuals. In case of significance in one-way ANOVA, Tukey's Honest Significant Difference (HSD) post-hoc test was utilized to compare conditions.

Causality was inferred using a one-sample two-tail t -test on net transfer entropy, with unknown variance and reference mean set to zero for each condition. Two-tail paired t -tests were also used to compare the first segments of each distance travelled and average absolute turn rate of the zebrafish with their relative last segments for each condition, paired for each trial.

Cumulative distributions of the distance of zebrafish from the center were analyzed through pairwise comparisons between the four conditions using the two-sample Kolmogorov-Smirnov test, and the p value needed to reach significance was adjusted using the Bonferroni method.

All the analyses were performed on R 3.3.2,⁵⁹ using "multcomp package 1.4-6"⁶⁰ for post-hoc analyses, and were conducted with a significance level set at 0.05.

III. RESULTS

A. Transfer entropy reveals differences in the information flow as the stimulus is varied

Transfer entropy from the stimulus to the focal subject did not vary as a function of the stimulus ($F_{2,25} = 1.07$, $p = 0.3589$) [Fig. 5(a)]. On the other hand, transfer entropy from the zebrafish to the stimulus varied depending on the condition ($F_{2,25} = 4.33$, $p = 0.0242$), with focal fish in Live condition transferring more information to the stimulus than focal subjects fish in the Replica condition ($p < 0.05$ in post-hoc tests).

The analysis of net transfer entropy did not indicate causal relationships between the stimulus and the zebrafish in CTRL Replica and Live conditions (CTRL Replica: $t_9 = -1.78$, $p = 0.1080$; Live: $t_9 = 1.90$, $p = 0.0900$) [Fig. 5(b)]. On the other hand, a net information flow was found in the Replica condition ($t_7 = -3.07$, $p = 0.0179$), with the stimulus causing the behavior of the focal subject. (Although CTRL Replica and Replica conditions shared a comparable average value for the net transfer entropy, data in the Replica condition were less variable among trials.)

As shown in Tables I and II, neither changing the number of bins nor down sampling the data hampers the ability of net transfer entropy to isolate information flow from the replica to the focal subject. Increasing the number of bins beyond five leads to a net information flow from the live stimulus to the focal subject in the Live condition. With respect to the CTRL Replica condition, only a number of bins equal to eight results in a net information flow from the stimulus to the fish (Fig. 6). Down sampling the data leads to a net transfer entropy in the CTRL Replica condition only with 10 fps (Fig. 7).

B. Locomotor activity and spatial distribution of zebrafish are not affected by the stimulus

The average distance travelled by zebrafish was not found to vary with the condition ($F_{3,34} = 1.83$, $p = 0.1604$), whereby focal subjects travelled an equivalent distance in the four conditions [Fig. 8(a)]. Similarly, the average

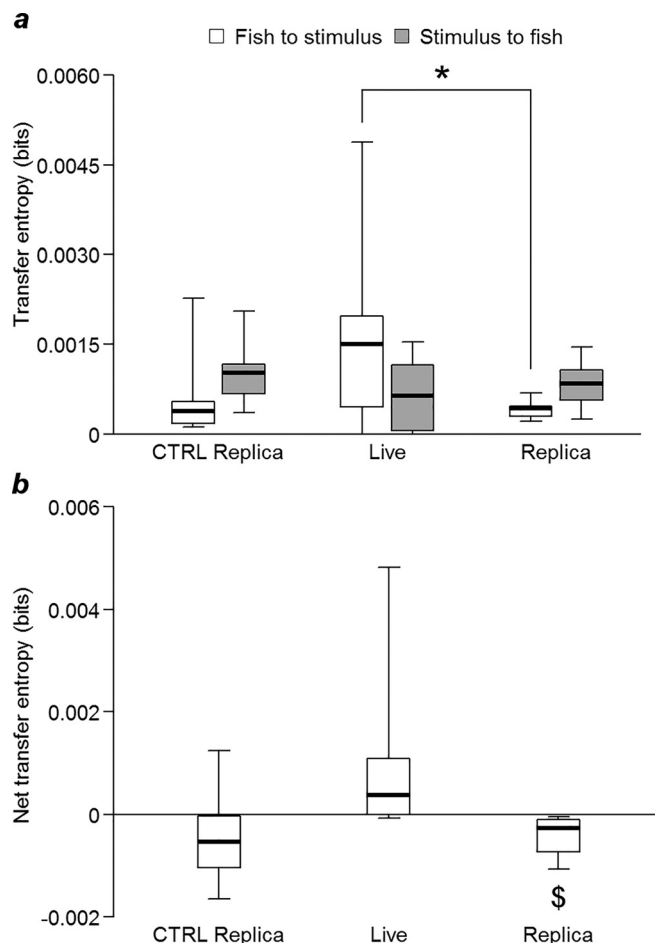


FIG. 5. Information flow from zebrafish to stimulus (white bars) and from stimulus to zebrafish (grey bars) (a) and net transfer entropy (black bars) (b). The bottom and top of each box are the first and third quartiles, the band inside the box is the median, and whiskers identify the entire distribution of the data. Bars and vertical lines with asterisks indicate statistically significant comparisons ($p < 0.05$) in post-hoc tests. The dollar symbol indicates a significant difference ($p < 0.05$) in the t -test comparison with zero.

TABLE I. Results of the t -test on the net transfer entropy in bits for variable number of bins at 30 fps.

Number of bins	CTRL Replica	Live	Replica
3	$t_9 = -2.07$, $p = 0.0676$	$t_9 = 1.65$, $p = 0.1338$	$t_7 = -2.36$, $p = 0.0496$
4	$t_9 = -1.78$, $p = 0.1080$	$t_9 = 1.90$, $p = 0.0900$	$t_7 = -3.07$, $p = 0.0179$
5	$t_9 = -1.23$, $p = 0.2484$	$t_9 = 1.73$, $p = 0.1171$	$t_7 = -3.71$, $p = 0.0075$
6	$t_9 = -1.57$, $p = 0.1497$	$t_9 = 2.28$, $p = 0.0481$	$t_7 = -3.34$, $p = 0.0123$
7	$t_9 = -1.25$, $p = 0.2441$	$t_9 = 2.53$, $p = 0.0320$	$t_7 = -5.01$, $p = 0.0015$
8	$t_9 = -2.74$, $p = 0.0226$	$t_9 = 3.19$, $p = 0.0110$	$t_7 = -3.57$, $p = 0.0091$
9	$t_9 = -1.67$, $p = 0.1287$	$t_9 = 1.63$, $p = 0.1365$	$t_7 = -6.46$, $p = 0.0003$
10	$t_9 = -1.71$, $p = 0.1221$	$t_9 = 2.96$, $p = 0.0159$	$t_7 = -6.10$, $p = 0.0005$

TABLE II. Results of the *t*-test on the net transfer entropy in bits for down sampled data with 4 bins.

Frame rate (fps)	CTRL Replica	Live	Replica
30	$t_9 = -1.78$, $p = 0.1080$	$t_9 = 1.90$, $p = 0.0900$	$t_7 = -3.07$, $p = 0.0179$
10	$t_9 = -2.40$, $p = 0.0396$	$t_9 = 1.61$, $p = 0.1404$	$t_7 = -2.76$, $p = 0.0280$
5	$t_9 = -1.98$, $p = 0.0785$	$t_9 = 1.90$, $p = 0.0897$	$t_7 = -2.81$, $p = 0.0260$
1	$t_9 = -1.96$, $p = 0.0821$	$t_9 = 0.70$, $p = 0.4989$	$t_7 = -3.10$, $p = 0.0173$

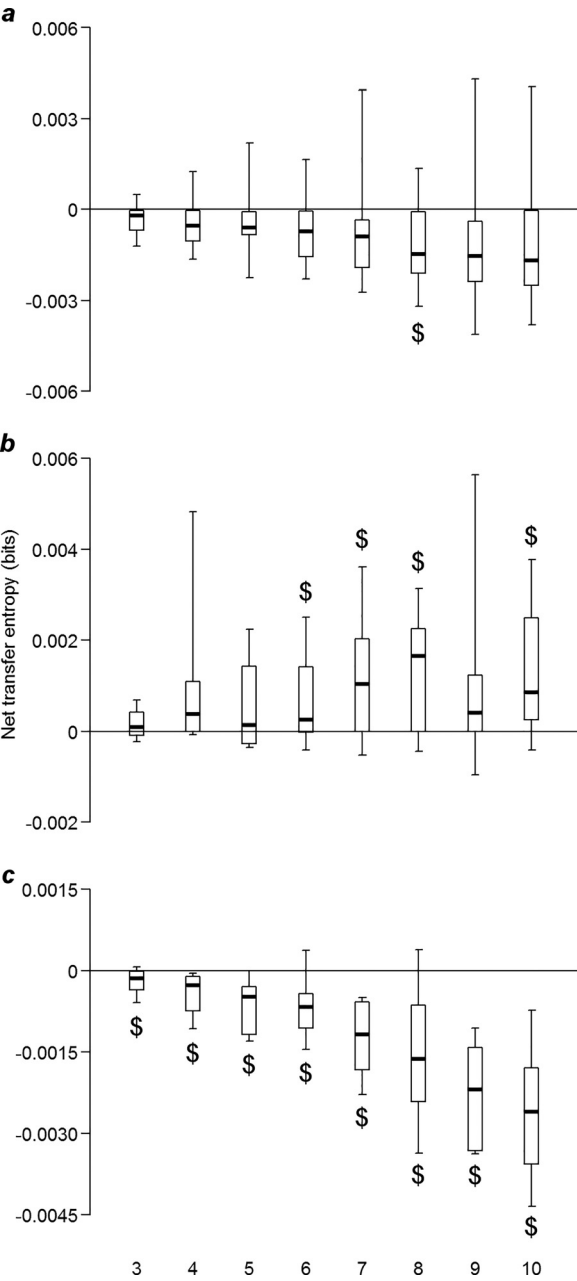


FIG. 6. Net transfer entropy for a number of bins from 3 to 10 for CTRL Replica (a), Live (b), and Replica conditions (c). The bottom and top of each box are the first and third quartiles, the band inside the box is the median, and whiskers identify the entire distribution of the data. The dollar symbol indicates a significant difference ($p < 0.05$) in the *t*-test comparison with zero.

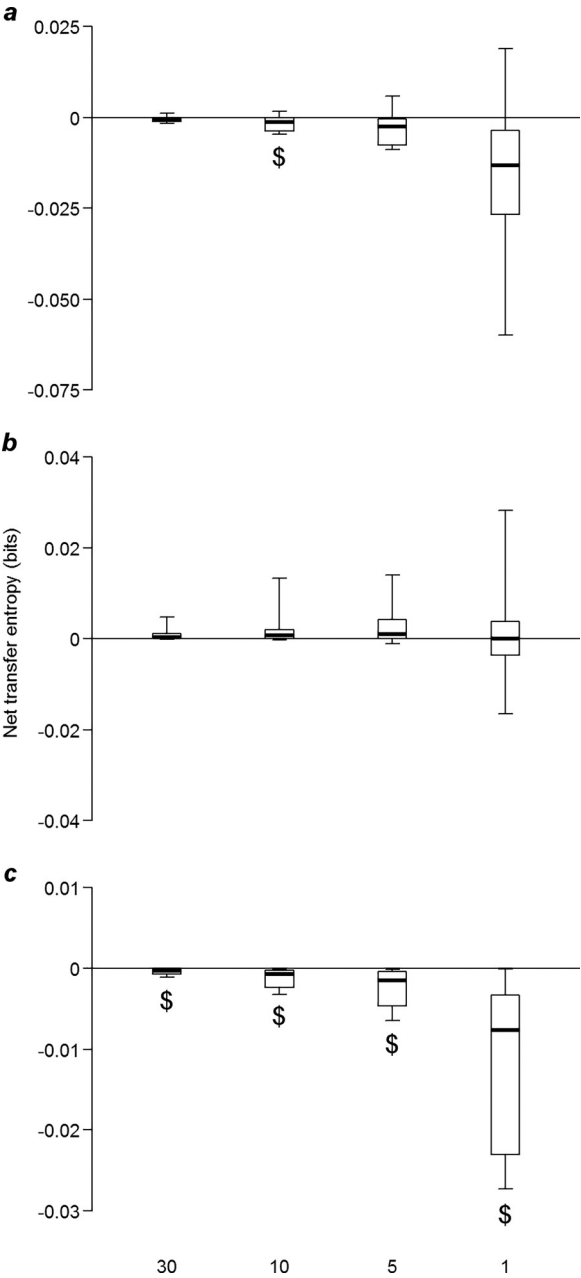


FIG. 7. Net transfer entropy for a range of values of sampling time from 30 to 1 fps for CTRL Replica (a), Live (b), and Replica conditions (c). The bottom and top of each box are the first and third quartiles, the band inside the box is the median, and whiskers identify the entire distribution of the data. The dollar symbol indicates a significant difference ($p < 0.05$) in the *t*-test comparison with zero.

absolute turn rate of zebrafish did not vary across the four conditions ($F_{3,34} = 1.45$, $p = 0.2456$) [Fig. 8(b)].

Although the cumulative distributions of the distance of zebrafish from the center of the stimulus tank may suggest a variation across conditions, especially in the comparison between Replica and Live conditions (Fig. 9), none of the comparisons reached statistical significance, as shown in Table III.

C. Locomotor activity of the live predator is influenced by the presence of the zebrafish

The analysis of the average distance travelled by the stimulus revealed that the live predator swam significantly

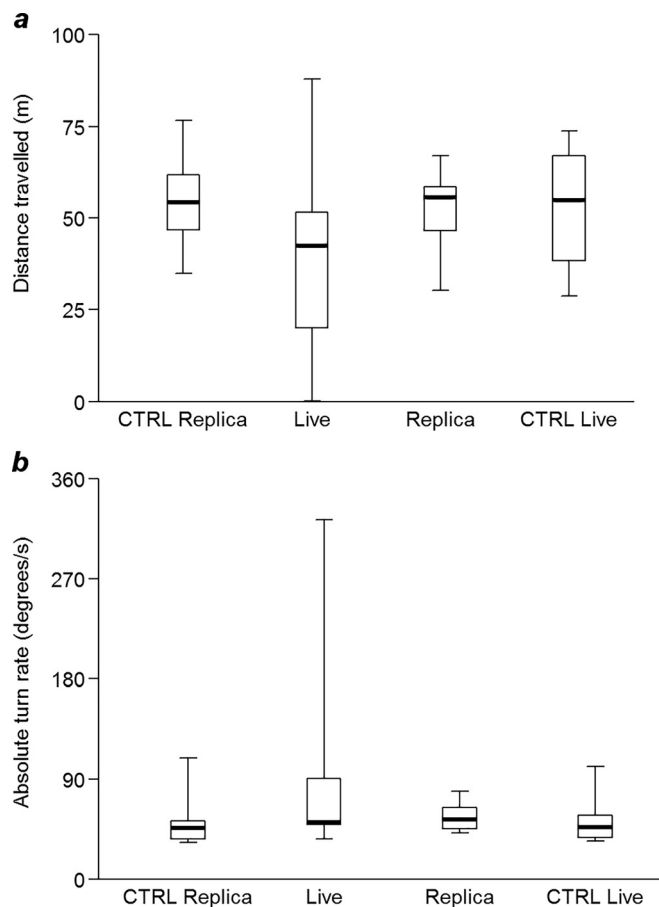


FIG. 8. Average distance travelled by zebrafish (a) and average absolute turn rate of zebrafish (b). The bottom and top of each box are the first and third quartiles, the band inside the box is the median, and whiskers identify the entire distribution of the data.

more than the robotic stimuli ($F_{2,25} = 6.33$, $p = 0.0059$) (Fig. 10).

D. Zebrafish tends to inspect the replica

The percentage of time spent outside of the predator area was affected by the stimulus ($F_{2,24} = 3.98$, $p = 0.0321$), with the Replica condition reporting lower values when compared to the Live condition ($p < 0.05$ in post-hoc tests) [Fig. 11(a)]. Similarly, the number of crossings of the predator area was significantly different among conditions ($\chi^2 = 32.79$, $p = 0.0175$). Post-hoc tests revealed a significant difference between Live and Replica conditions [Fig. 11(b)], with the zebrafish in the Replica condition entering the predator area more frequently.

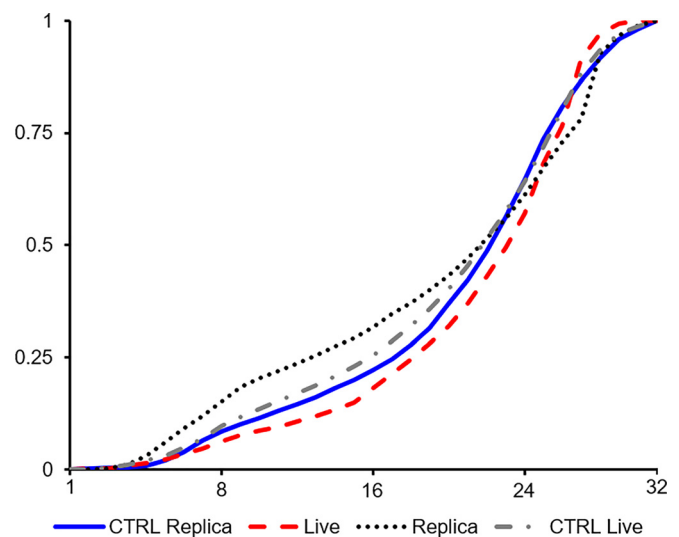


FIG. 9. Cumulative distributions of the distance by zebrafish from the center of the tank. The blue solid line represents CTRL Replica condition, the red dashed line represents Live condition, the black dotted line represents Replica condition, and the grey dashed-dotted line represents CTRL Live condition.

E. The effects of the live predator on zebrafish activity change in time

Comparisons between the first and the last segments of the trials indicated that the zebrafish in the Live condition travelled on average significantly more during the last segment ($t_9 = -2.59$, $p = 0.0290$) [Fig. 12(a)]. No significant differences were observed for CTRL Replica ($t_9 = -1.72$, $p = 0.1200$), Replica ($t_7 = 2.11$, $p = 0.0731$), and CTRL Live ($t_9 = -1.87$, $p = 0.0932$) conditions. Although we found the p value close to significance, the average absolute turn rate of the zebrafish did not vary between the first and last segments for the Live condition ($t_9 = 2.05$, $p = 0.0708$) [Fig. 12(b)]. No differences were also registered for CTRL Replica ($t_9 = 1.23$, $p = 0.2507$), Replica ($t_7 = 1.59$, $p = 0.1560$), or CTRL Live ($t_9 = 1.59$, $p = 0.1466$) conditions.

IV. DISCUSSION

Transfer entropy holds promise to advance our understanding of animal behavior, by offering a data-driven, model-free approach to quantify causal relationships from raw time series. Given two stochastic systems, transfer entropy may be used to infer a causal relationship between them as a net information flow, such that the uncertainty in the prediction of the future of one system is reduced based on the past of the other.¹⁸ In this study, we demonstrated the

TABLE III. Results of the Kolmogorov-Smirnov test for each pairwise comparison.

	CTRL Replica	Live	Replica	CTRL Live
CTRL Replica
Live	$D = 0.09$, $p = 0.9993$
Replica	$D = 0.19$, $p = 0.6351$	$D = 0.25$, $p = 0.2730$
CTRL Live	$D = 0.06$, $p = 1$	$D = 0.16$, $p = 0.8378$	$D = 0.12$, $p = 0.9683$...

Note that the critical p value needed to reach statistical significance in this analysis was 0.0083 (Bonferroni's method for six comparisons with $\alpha = 0.05$).

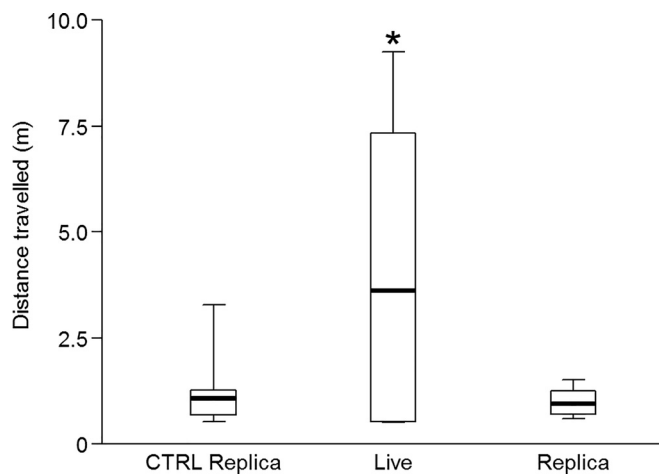


FIG. 10. Average distance travelled by the stimulus. The bottom and top of each box are the first and third quartiles, the band inside the box is the median, and whiskers identify the entire distribution of the data. Asterisk indicates a significant difference in post-hoc tests ($p < 0.05$) with respect to the other conditions.

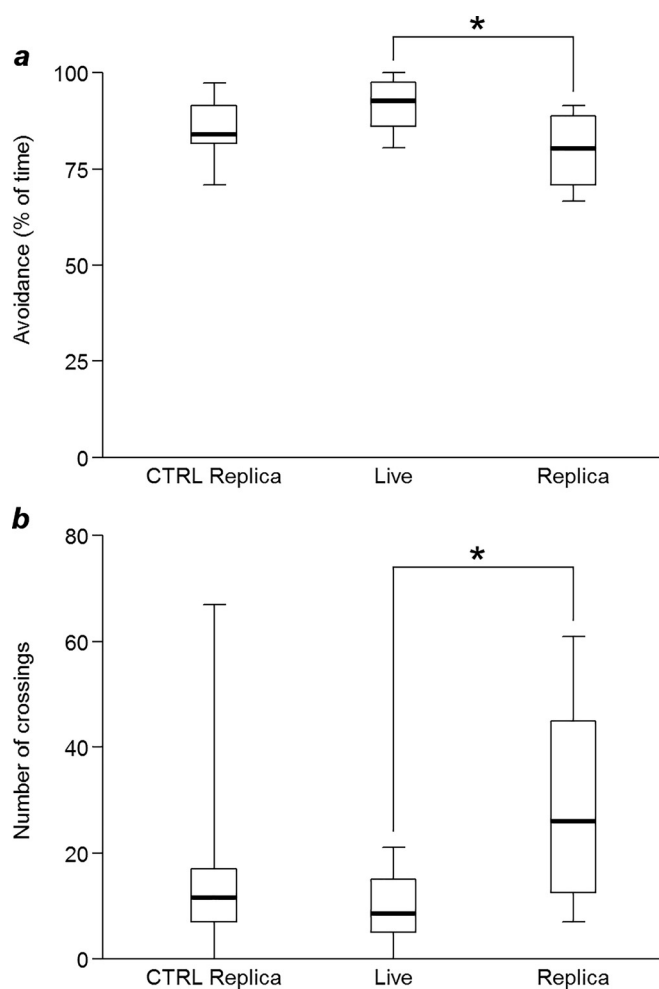


FIG. 11. Average avoidance of the stimulus by zebrafish (a) and average number of crossings by zebrafish (b). The bottom and top of each box are the first and third quartiles, the band inside the box is the median, and whiskers identify the entire distribution of the data. Bars and vertical lines with asterisks indicate statistically significant comparisons ($p < 0.05$) in post-hoc tests.

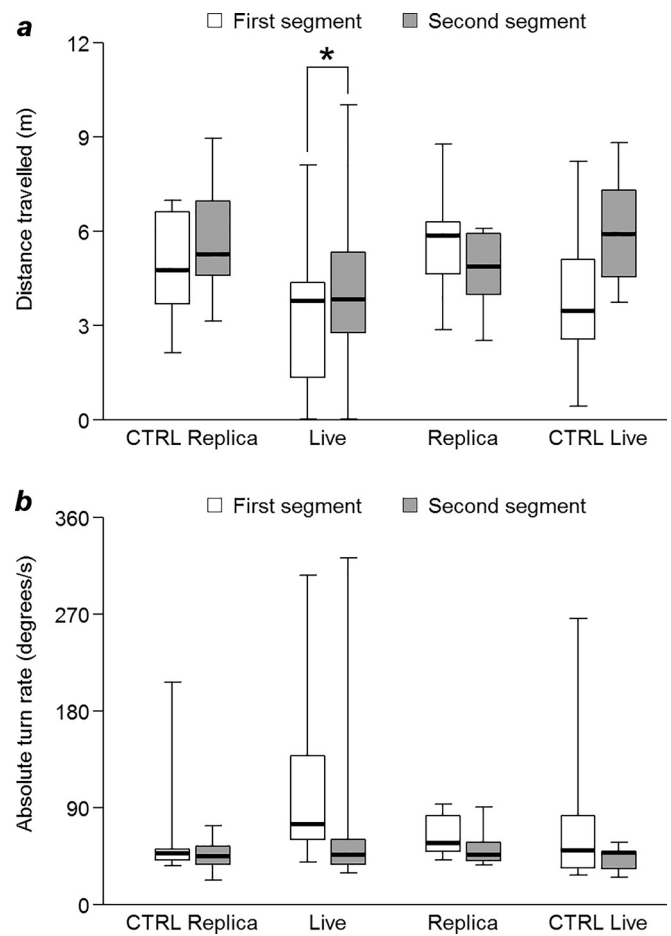


FIG. 12. Comparisons between first (white boxplot) and last segments (grey boxplot) of the travelled distance by zebrafish (a) and absolute turn rate of the zebrafish (b). The bottom and top of each box are the first and third quartiles, the band inside the box is the median, and whiskers identify the entire distribution of the data. Bars and vertical lines with asterisks indicate significant difference ($p < 0.05$) in the t -test.

validity of this information-theoretic construct in the context of predator-prey interactions. By leveraging recent advancements in the use of robotic stimuli in animal behavior,^{33–38} we established a novel robotic platform to elicit a controlled fear response in zebrafish.

The platform integrated a robotic replica, designed after the morpho-physiology of a zebrafish predator, which was actuated along preprogrammed trajectories to establish a controlled one-directional information flow. In this engineered one-directional information flow, the motion of the predator was independent of the response of the prey. In line with our expectations, transfer entropy was able to isolate the causal relationship underlying experimental observations. From the analysis of the time series of the position of the focal subjects and the robotic stimulus, we identified a robust one-directional information flow from stimulus to zebrafish.

Neither changing the number of bins nor downsampling the data hindered the ability of transfer entropy to identify the underlying cause-and-effect relationship, whereby we consistently recorded a significant information flow from the replica to the fish for all the explored combinations of the parameters. Although some of these combinations considerably

strained the estimation of the probability density functions in the computation of transfer entropy, a false reading was never documented. Specifically, increasing the number of bins to 10 led to a total of 1000 combinations for the joint probability density function, with only a dataset of 18000 frames. Similarly, down sampling the data to 1 fps resulted in a dataset of 600 frames, from which we estimated a probability density function with 64 combinations (4^3).

This net information flow was partially mitigated when the robotic stimulus was replaced by a moving transparent rod. Specifically, utilizing four bins and the full resolution of the video, we did not detect an information flow between the moving rod and the focal subject, suggesting that the visual appearance of the replica was a determinant of zebrafish response. This evidence is in agreement with our previous work,³⁹ which indicated that the presentation of a replica of the red tiger oscar constitutes a robust fear-evoking stimulus. However, we acknowledged a flow of information from the moving rod to the focal subjects when down sampling to 10 fps or increasing the number of bins to eight. The large values of the number of bins and the moderate sampling rates at which this information flow is detected strain the applicability of transfer entropy, due to the limited number of samples available for estimating each possible value of the joint probability density. We cannot dismiss the possibility that the motion of the transparent rod influenced the behavior of the subject, which might have perceived the movement of the water generated by the rod in the stimulus tank.

The ability of transfer entropy to detect a known information flow in the interactions between a robotic stimulus and zebrafish was also demonstrated in some of our previous work.^{61–64} In this series of papers, we examined the response of zebrafish to a replica, designed after a single or a shoal of conspecifics, in an effort to clarify the determinants of social behavior. Experiments were conducted in a binary preference test, where the robotic replica was actuated along preprogrammed one-,^{61,64} two-,⁶³ or three-dimensional⁶² trajectories by a robotic platform. In these studies, transfer entropy was scored in terms of the linear position of the focal fish and the replica along the short-axis of the tank from a top view. Through this information-theoretic construct, these studies have helped clarify the role of the size and motion of the replica in zebrafish response and illustrated the possibility of modulating the interaction through psychoactive compounds. The present study strengthens the potential of transfer entropy by demonstrating for the first time its use in the study of predator-prey interactions. Different from our previous work,^{61–64} the replica considered in this study elicits a controlled fear response, which we sought to isolate through the computation of transfer entropy.

Upon validation of transfer entropy in the controlled robotics-based experiment, we examined the interactions between a live red tiger oscar and a zebrafish in the same setup. Transfer entropy did not robustly identify a direction of information flow in the presence of a live predator for all the entirety of the parameter combinations. Specifically, we detected a significant net information flow from the live fish to the predator for larger numbers of bins, but for smaller bins statistical significance was lost. Also, we reported a

significant increase in the transfer entropy from the focal subject to the stimulus with respect to the condition in which we used the preprogrammed robotic replica. Thus, it is plausible that the visual feedback from the live stimulus played a role in these results, accounting for an increased responsiveness of the predator to the zebrafish movement. This evidence is in partial disagreement with experiments by Hu *et al.*,²⁹ where it was proposed that a net information flow was found from a predator (northern snakehead) to a prey (rosy bitterling) fish in a similar circular arena.

We put forward two aspects to explain this discrepancy. First, our study was based on a different experimental setup compared to Hu *et al.*,²⁹ where the predator fish was swimming in the outer portion of the circular arena rather than in the inner stimulus tank. As a result, the prey fish in our experiment was given a wider region to swim and exhibit escape responses. The experimental time allocated for the study of Hu *et al.*²⁹ was also vastly different than ours, whereby their experiment consisted of one hour of observation, following eight hours of acclimatization for the predator. In our experiments, the fish were given 10 min to habituate to the environment and we scored their behavior for the following 10 min. The differences in the allotted habituation and experimental times might explain a change in the responsiveness of the predator, which would then manifest into a variation in the direction of information flow.

Second, different from other “active and cruising” predators,^{4,5} the red tiger oscar fish displays a “sit-and-wait” attack strategy,⁶⁵ which is a common foraging behavior among Central and South American large cichlid predators.^{66,67} Based on its color pattern and camouflage skills, this type of predator generally hides and waits for the ideal moment to leap on its prey with a fast, straight-forward, startle movement. Although our experimental setup did not fully replicate the habitat of this predatory fish, it is tenable to hypothesize that its natural hunting instincts played a role in the behavior we observed. Considering the relative small size of the stimulus tank, it might be suggested that the red tiger oscar fish preferred to sit on a spot and move toward the zebrafish whenever it approached, rather than continuously swimming.

A complementary line of research to offer validation for the use of transfer entropy in studying predator-prey interactions could entail interactive experiments.³³ Similar to previous efforts,^{68–71} the robotic replica would be actuated based on the real-time feedback from the live subjects. In this case, one could theoretically reverse the direction of information flow that we registered in our experiments, such that the motion of the robotic stimulus would be influenced by the live subject and not the other way around. For example, we may consider the possibility of a robotic replica that would integrate a simulated predatory attack in its motion, by quickly accelerating toward an approaching focal subject. Alternatively, the replica may be concealed and suddenly move toward the focal fish, thereby simulating the natural sit-and-wait attack strategy of red tiger oscar fish.⁶⁵ Two major technical advancements should be pursued to achieve this ambitious goal, that is: (i) real-time tracking of the live animal and (ii) fast actuation of the robotic stimulus

along complex, biologically inspired locomotory patterns. Addressing these technical challenges will be the objective of future research, requiring significant progress in both computer vision and robotics.

Comparing the response of zebrafish to the live and robotic stimulus, we note that zebrafish spent more time close to the robotic replica and displayed more instances of shuttling back and forth from the predator area. We propose that these behavioral patterns represented instances of “predator inspection.”^{51,72} Since the robotic replica was unresponsive to zebrafish movement, we may propose that focal subjects would tend to inspect more this novel stimulus than the live predator, which instead reacted to the zebrafish approaches. The reactivity of the predator to the zebrafish is also confirmed by the larger distance travelled by the predator in response to potential prey. While in the pilot studies, the predators travelled 124.6 cm over 10 min, this distance doubled in the presence of zebrafish, confirming a direct influence of zebrafish behavior on the predator response. An alternative explanation for the observed difference in the time spent close to the stimulus might be sought in a limited degree of biomimicry of the replica, although the increased number of excursions in the predator area does not support this possibility.

The difference in the avoidance response of zebrafish toward the live and robotic stimuli was accompanied by a trend in the locomotor activity. Although the distance travelled by zebrafish and its absolute turn rate did not significantly vary across conditions, zebrafish reduced their distance travelled in the presence of the live predator and data analysis suggested a nearly significant increase in the average absolute turn rate with respect to the other conditions. This trend was echoed in the cumulative distribution of the distance from the center of the tank, where qualitative differences could be noted in the response of zebrafish to a live predator. We should acknowledge that, although our analysis did not reveal a statistically significant difference among groups, it is tenable to hypothesize that a larger number of experimental subjects could have improved our statistical power, thereby leading to a significant result in the average distance travelled and average absolute turn rate. The potential increase in the average absolute turn rate is compatible with sudden escape maneuvers evoked by the interaction with the live predator. Similarly, the decrease in the travelled distance could be associated with a reduction in predator inspections, causing the subjects to swim a smaller distance in the circular arena.

The analysis of time effects in the activity of zebrafish mirrored previous work in the use of robots for hypothesis-driven research which demonstrated the consistency of the response of zebrafish to robotic stimuli.^{39,73} The increase in the distance travelled toward the end of the trial might be interpreted as a reduction in the emotional value of the stimulus caused by the presence of the separating wall. After sufficient time, zebrafish might apprehend the limited predation risk constituted by the live predator, thereby increasing the distance swam in the circular arena. An alternative explanation could be proposed on the basis of increased distress of the predators throughout the trials. Since we used only two

different live predators, it may be possible that the repeated handling of the fish could have caused an increased stress response hampering their behavioral output. Although a live predator could be identified as the most natural representation of a fear stimulus for a prey, it is not exempt from several biases. Fatigue, tiredness, and idiosyncrasies between subjects might interfere with predator-prey interactions, resulting in a high variability and low reproducibility among experimental trials.^{39,73}

This study posits the integration of information theory and robotics to improve our understanding of predator-prey interactions. The key methodological contribution of the work is the development of a novel robotics-based platform to engineer the direction of information flow in predator-prey interactions. Previous work on the use of fear-evoking robotic stimuli^{39,40} was limited to static replicas, which were not able to maneuver in the experimental tank. This study puts forward a first, moving robotic stimulus for use in experiments in fear and anxiety response of zebrafish. Future work should seek to further expand on the platform to enable more complex three-dimensional motion patterns and potentially afford interactivity through closed-loop control.

From a theoretical point of view, we demonstrated the validity of transfer entropy to help isolate the known cause-and-effect relationship from the time series of the motion of the predator and prey and leveraged this knowledge in the study of the interaction between a live predator and a zebrafish. This experimental evidence contributes to the growing literature on the use of transfer entropy to unravel causal relationships across science and engineering,¹⁸ offering a practical assessment in the analysis of predator-prey interactions. Further work should explore the design of robotics-based experiments to support an improved understanding of the subtle differences between predictive transfer and causal information flow.⁷⁴ Also, future studies should seek to explore the application of transfer entropy to reconstruct information flow during predator attacks, where social interactions among prey mediate and support the spreading of information about the attack.^{2,75,76}

SUPPLEMENTARY MATERIAL

See [supplementary material](#) for videos 1–5. Video 1: The sample video shows 45 s of one trial for condition Live, in which zebrafish is presented as a live predator. The video is from the top view camera. Video 2: The sample video shows 45 s of the red tiger oscar in the stimulus tank during one trial for the condition Live. The video is from the camera in the stimulus tank. Video 3: The sample video shows 45 s of one trial for condition CTRL Live, in which no stimulus was presented to zebrafish. The video is from the top view camera. Video 4: The sample video shows 45 s of one trial for condition Replica, in which zebrafish is presented the robotic platform with a replica of the red tiger oscar attached to it. The video is from the top view camera. Video 5: The sample video shows 45 s of one trial for condition CTRL Replica, in which zebrafish is presented the robotic platform with no replica attached. The video is from the top view camera.

ACKNOWLEDGMENTS

This work was supported by the National Science Foundation under Grant No. CMMI-1433670 and Grant No. CMMI-1505832. The authors are grateful to Violet Mwaffo for help in the analysis of the data. T.R. and M.P. designed the research; D.N., T.R., and G.C.C. performed the experiments; D.N., T.R., and G.C.C. scored animal behavior; D.N., T.R., and M.P. performed statistical analyses; and D.N., T.R., and M.P. wrote the manuscript. Datasets and codes used in the analyses are stored at the authors' home institution and will be provided on request. Correspondence and requests for materials should be addressed to M.P. (mporfiri@nyu.edu).

The authors declare no competing financial interests.

- ¹S. R. Dall, L.-A. Giraldeau, O. Olsson, J. M. McNamara, and D. W. Stephens, *Trends Ecol. Evol.* **20**(4), 187–193 (2005).
- ²S. J. Shettleworth, *Anim. Behav.* **61**(2), 277–286 (2001).
- ³M. Stevens, *Sensory Ecology, Behaviour, and Evolution* (Oxford University Press, 2013).
- ⁴P. Webb, *Am. Zool.* **24**(1), 107–120 (1984).
- ⁵P. J. Hart, *The Behaviour of Teleost Fishes* (Springer, 1986), pp. 211–235.
- ⁶A. E. Magurran and A. Higham, *Ethology* **78**(2), 153–158 (1988).
- ⁷N. Abaid, S. Butail, M. Porfiri, and D. Spinello, *Eur. Phys. J.: Spec. Top.* **224**(17), 3109–3117 (2015).
- ⁸D. J. Sumpter, *Collective Animal Behavior* (Princeton University Press, 2010).
- ⁹J. Krause, R. James, D. Franks, and D. P. Croft, *Animal Social Networks* (Oxford University Press, USA, 2014).
- ¹⁰B. C. Downing and N. J. Royle, *Animal Social Networks* (John Wiley & Son, Chichester, UK, 2013).
- ¹¹N. Pinter-Wollman, E. A. Hobson, J. E. Smith, A. J. Edelman, D. Shizuka, S. D. Silva, J. S. Waters, S. D. Prager, T. Sasaki, and G. Wittemyer, *Behav. Ecol.* **25**(2), 242–255 (2013).
- ¹²T. M. Cover and J. A. Thomas, *Elements of Information Theory* (John Wiley & Sons, 2012).
- ¹³C. E. Shannon and W. Weaver, *The Mathematical Theory of Information* (University of Illinois Press, Urbana, IL, 1949).
- ¹⁴M. P. Paulus, M. A. Geyer, L. H. Gold, and A. J. Mandell, *Proc. Natl. Acad. Sci. U.S.A.* **87**(2), 723–727 (1990).
- ¹⁵B. McCowan, S. F. Hanser, and L. R. Doyle, *Anim. Behav.* **57**(2), 409–419 (1999).
- ¹⁶J. S. Avery, *Information Theory and Evolution* (World Scientific, 2012).
- ¹⁷K. Hlaváčková-Schindler, M. Paluš, M. Vejmelka, and J. Bhattacharya, *Phys. Rep.* **441**(1), 1–46 (2007).
- ¹⁸T. Bossomaier, L. Barnett, M. Harré, and J. T. Lizier, *An Introduction to Transfer Entropy: Information Flow in Complex Systems* (Springer, 2016).
- ¹⁹O. Stetter, D. Battaglia, J. Soriano, and T. Geisel, *PLoS Comput. Biol.* **8**(8), e1002653 (2012).
- ²⁰R. Vicente, M. Wibral, M. Lindner, and G. Pipa, *J. Comput. Neurosci.* **30**(1), 45–67 (2011).
- ²¹J. Hlinka, D. Hartman, M. Vejmelka, J. Runge, N. Marwan, J. Kurths, and M. Paluš, *Entropy* **15**(6), 2023–2045 (2013).
- ²²J. Runge, J. Heitzig, V. Petoukhov, and J. Kurths, *Phys. Rev. Lett.* **108**(25), 258701 (2012).
- ²³L. Sandoval, *Entropy* **16**(8), 4443–4482 (2014).
- ²⁴L. Faes, D. Marinazzo, A. Montalto, and G. Nollo, *IEEE Trans. Biomed. Eng.* **61**(10), 2556–2568 (2014).
- ²⁵C. Grabow, J. Macinko, D. Silver, and M. Porfiri, *Chaos* **26**(8), 083113 (2016).
- ²⁶R. P. Anderson, G. Jimenez, J. Y. Bae, D. Silver, J. Macinko, and M. Porfiri, *SIAM J. Appl. Dyn. Syst.* **15**(3), 1384–1409 (2016).
- ²⁷T. Schreiber, *Phys. Rev. Lett.* **85**(2), 461 (2000).
- ²⁸N. Orange and N. Abaid, *Eur. Phys. J.: Spec. Top.* **224**(17–18), 3279–3293 (2015).
- ²⁹F. Hu, L. J. Nie, and S. J. Fu, *Entropy* **17**(10), 7230–7241 (2015).
- ³⁰Y. Sun, L. F. Rossi, C. C. Shen, J. N. Miller, X. R. Wang, J. T. Lizier, M. Prokopenko, and U. Senanayake, e-print [arXiv:1407.0007](https://arxiv.org/abs/1407.0007).
- ³¹X. R. Wang, J. M. Miller, J. T. Lizier, M. Prokopenko, and L. F. Rossi, *PLoS One* **7**(7), e40084 (2012).
- ³²M. S. Baptista, R. M. Rubinger, E. R. Viana, J. C. Sartorelli, U. Parlitz, and C. Grebogi, *PLoS One* **7**(10), e46745 (2012).
- ³³J. Krause, A. F. Winfield, and J. L. Deneubourg, *Trends Ecol. Evol.* **26**(7), 369–375 (2011).
- ³⁴B. A. Klein, J. Stein, and R. C. Taylor, *Commun. Integr. Biol.* **5**(5), 466–472 (2012).
- ³⁵S. Butail, N. Abaid, S. Macri, and M. Porfiri, in *Robot Fish* (Springer, 2015), Part IV, pp. 221–240.
- ³⁶J. A. Carr, *Front. Neurosci.* **9**, 414 (2015).
- ³⁷S. Mitri, S. Wischmann, D. Floreano, and L. Keller, *Biol. Rev.* **88**(1), 31–39 (2013).
- ³⁸A. Frohnwieser, J. C. Murray, T. W. Pike, and A. Wilkinson, *J. Exp. Anal. Behav.* **105**(1), 14–22 (2016).
- ³⁹F. Ladu, T. Bartolini, S. G. Panitz, F. Chiarotti, S. Butail, S. Macri, and M. Porfiri, *Zebrafish* **12**(3), 205–214 (2015).
- ⁴⁰V. Cianca, T. Bartolini, M. Porfiri, and S. Macri, *PLoS One* **8**(7), e69661 (2013).
- ⁴¹L. I. Zon and R. T. Peterson, *Nat. Rev. Drug Discov.* **4**(1), 35–44 (2005).
- ⁴²D. J. Grunwald and J. S. Eisen, *Nat. Rev. Genet.* **3**(9), 717–724 (2002).
- ⁴³R. White, K. Rose, and L. Zon, *Nat. Rev. Cancer* **13**(9), 624–636 (2013).
- ⁴⁴A. M. Stewart, J. F. Ullmann, W. H. Norton, M. Parker, C. Brennan, R. Gerlai, and A. V. Kalueff, *Mol. Psychiatry* **20**(1), 2–17 (2015).
- ⁴⁵A. V. Kalueff, D. J. Echevarria, and A. M. Stewart, *Prog. Neuro-Psychopharmacol. Biol. Psychiatry* **55**, 1–6 (2014).
- ⁴⁶R. Gerlai, *Evol. Psychol.* **11**(3), 591–605 (2013).
- ⁴⁷C. T. Gross and N. S. Canteras, *Nat. Rev. Neurosci.* **13**(9), 651–658 (2012).
- ⁴⁸J. LeDoux, *Neuron* **73**(4), 653–676 (2012).
- ⁴⁹S. L. Bass and R. Gerlai, *Behav. Brain Res.* **186**(1), 107–117 (2008).
- ⁵⁰L. J. G. Barcellos, F. Ritter, L. C. Kreutz, R. M. Quevedo, L. B. da Silva, A. C. Bedin, J. Finco, and L. Cericato, *Aquaculture* **272**(1), 774–778 (2007).
- ⁵¹L. A. Dugatkin, M. A. McCall, R. G. Gregg, A. Cavanaugh, C. Christensen, and M. Unseld, *Ethol. Ecol. Evol.* **17**(1), 77–81 (2005).
- ⁵²R. Gerlai, *Behav. Brain Res.* **207**(2), 223–231 (2010).
- ⁵³G. M. Cahill, *Brain Res.* **708**(1), 177–181 (1996).
- ⁵⁴T. Bartolini, S. Butail, and M. Porfiri, *Environ. Biol. Fishes* **98**(3), 825–832 (2015).
- ⁵⁵B. L. Ruddell and P. Kumar, *Water Resour. Res.* **45**(3), W03420, doi:10.1029/2008WR007280 (2009).
- ⁵⁶V. Mwaffo, S. Butail, M. Di Bernardo, and M. Porfiri, *Zebrafish* **12**(3), 250–254 (2015).
- ⁵⁷G. Polverino, D. Bierbach, S. Killen, S. Uusi-Heikkilä, and R. Arlinghaus, *J. Fish Biol.* **89**(5), 2251–2267 (2016).
- ⁵⁸W. C. Navidi, *Statistics for Engineers and Scientists* (McGraw-Hill New York, 2006).
- ⁵⁹R Core Team, *R: A language and environment for statistical computing* (R Foundation for Statistical Computing, Vienna, Austria, 2016).
- ⁶⁰T. Hothorn, F. Bretz, and P. Westfall, *Biom. J.* **50**(3), 346–363 (2008).
- ⁶¹T. Bartolini, V. Mwaffo, A. Showler, S. Macri, S. Butail, and M. Porfiri, *Bioinspiration Biomimetics* **11**(2), 026003 (2016).
- ⁶²T. Ruberto, V. Mwaffo, S. Singh, D. Neri, and M. Porfiri, *R. Soc. Open Sci.* **3**(10), 160505 (2016).
- ⁶³S. Butail, F. Ladu, D. Spinello, and M. Porfiri, *Entropy* **16**(3), 1315–1330 (2014).
- ⁶⁴F. Ladu, V. Mwaffo, J. Li, S. Macri, and M. Porfiri, *Behav. Brain Res.* **289**, 48–54 (2015).
- ⁶⁵M. Tavares-Dias, T. J. S. M. Sousa, and L. R. Neves, *Biosci. J.* **30**(2), 546–555 (2014).
- ⁶⁶M. Tobler, *J. Fish Biol.* **66**(3), 877–881 (2005).
- ⁶⁷F. Z. Gibran and J. Armbruster, *Copeia* **2004**(2), 403–405.
- ⁶⁸D. T. Swain, I. D. Couzin, and N. E. Leonard, *Proc. IEEE* **100**(1), 150–163 (2012).
- ⁶⁹V. Kopman, J. Laut, G. Polverino, and M. Porfiri, *J. R. Soc. Interface* **10**(78), 20120540 (2013).
- ⁷⁰T. Landgraf, D. Bierbach, H. Nguyen, N. Muggelberg, P. Romanczuk, and J. Krause, *Bioinspiration Biomimetics* **11**(1), 015001 (2016).

- ⁷¹T. Landgraf, H. Nguyen, J. Schröer, A. Szengel, R. J. Clément, D. Bierbach, and J. Krause, *Biomimetic and Biohybrid Systems* (Springer International Publishing, 2014), pp. 178–189.
- ⁷²T. Pitcher, D. Green, and A. Magurran, *J. Fish Biol.* **28**(4), 439–448 (1986).
- ⁷³C. Spinello, S. Macrì, and M. Porfiri, *Alcohol* **47**(5), 391–398 (2013).
- ⁷⁴J. T. Lizier and M. Prokopenko, *Eur. Phys. J. B-Condens. Matter Complex Syst.* **73**(4), 605–615 (2010).
- ⁷⁵C. Brown and K. N. Laland, *Fish Fish.* **4**(3), 280–288 (2003).
- ⁷⁶J. W. Bradbury and S. L. Vehrencamp, *Principles of Animal Communication* (Sinauer Associates, Inc., Sunderland, MA, 1998).